

Contents lists available at ScienceDirect

## **Organic Geochemistry**

journal homepage: www.elsevier.com/locate/orggeochem



# Empowering conventional Rock-Eval pyrolysis for organic matter characterization of the siderite-rich sediments of Lake Towuti (Indonesia) using End-Member Analysis



Luis Ordoñez <sup>a</sup>, Hendrik Vogel <sup>b</sup>, David Sebag <sup>c,d</sup>, Daniel Ariztegui <sup>a</sup>, Thierry Adatte <sup>e</sup>, James M. Russell <sup>f</sup>, Jens Kallmeyer <sup>g</sup>, Aurèle Vuillemin <sup>a,h</sup>, André Friese <sup>g</sup>, Sean A. Crowe <sup>i</sup>, Kohen W. Bauer <sup>i</sup>, Rachel Simister <sup>i</sup>, Cynthia Henny <sup>j</sup>, Sulung Nomosatryo <sup>j</sup>, Satria Bijaksana <sup>k</sup>, the Towuti Drilling Project Scientific Team

#### ARTICLE INFO

Article history:
Received 14 January 2019
Received in revised form 17 April 2019
Accepted 2 May 2019
Available online 8 May 2019

Keywords: Thermal analysis Rock-Eval pyrolysis Organic matter Siderite Mineral carbon Tropical lake End-Member Analysis

#### ABSTRACT

Qualitative and quantitative changes of organic and carbonate carbon in sedimentary records are frequently used to reconstruct past environments, paleoproductivity and sediment provenance. Amongst the most commonly used proxies are Total Organic Carbon (TOC), Mineral Carbon (MinC), as well as Hydrogen (HI) and Oxygen Indices (OI) of organic matter (OM). Rock Eval pyrolysis enables the assessment of these quantitative and qualitative parameters with a single analysis. This is achieved through transient pyrolysis of the samples up to 650 °C followed by combustion up to 850 °C, with hydrocarbons, CO and CO<sub>2</sub> measured during the thermal decomposition of both OM and carbonate minerals.

Carbonate minerals with low thermal cracking temperatures, such as siderite (<400 °C), can induce significant matrix effects which bias the TOC, MinC and OI Rock-Eval parameters. Here we assess the applicability of End-Member Analysis (EMA) as a means of correcting Rock-Eval thermograms for siderite matrix effects. For this, we performed Rock-Eval pyrolysis on sideritic sediments of Lake Towuti (Indonesia). New thermal boundaries were constrained in Rock-Eval thermograms using EMA to limit siderite matrix effects and improve TOC, MinC and OI calculations. Our approach allowed us to: (1) evaluate the influence of siderite matrix effects on Rock-Eval thermograms; (2) properly exploit a Rock-Eval dataset to characterize the type and sources of OM in siderite-rich sediments and (3) identify the OM behind degradation and mineralization processes. The Rock-Eval dataset revealed sediments with a substantial amount of refractory OM, especially in those where TOC is high and HI characteristic of autochthonous biomass. These results, associated to alternative indices used to assess OM preservation, suggest that refractory OM is residually enriched following strong degradation of labile compounds. Finally, relatively labile and refractory organic fractions may be consumed in the formation of siderite during this sequential process of OM mineralization.

© 2019 The Authors. Published by Elsevier Ltd. This is an open access article under the CC BY-NC-ND license (http://creativecommons.org/licenses/by-nc-nd/4.0/).

#### 1. Introduction

Sedimentary organic matter (OM) in marine and lacustrine sedimentary records is widely used as an indicator of changes in past

depositional environments. Changes in OM quality and amounts can indicate the sources (aquatic/terrestrial) of sedimentary OM, the paleoecology (e.g., productivity) of aquatic systems, and help to identify the external drivers (climate, anthropogenic) leading

<sup>&</sup>lt;sup>a</sup> Department of Earth Sciences, University of Geneva, 1205 Geneva, Switzerland

<sup>&</sup>lt;sup>b</sup> Institute of Geological Sciences and Oeschger Centre for Climate Change Research, University of Bern, 3012 Bern, Switzerland

<sup>&</sup>lt;sup>c</sup> Normandie Univ, UNIROUEN, UNICAEN, CNRS, M2C, 76000 Rouen, France

<sup>&</sup>lt;sup>d</sup> Institute of Earth Surface Dynamics, Geopolis, University of Lausanne, Lausanne, Switzerland

<sup>&</sup>lt;sup>e</sup> Institut des Sciences de la Terre (ISTE), Université de Lausanne, GEOPOLIS, CH-1015 Lausanne, Switzerland

<sup>&</sup>lt;sup>f</sup>Department of Earth, Environmental, and Planetary Sciences, Brown University, Providence, RI 02912, USA

g GFZ German Research Centre For Geosciences, Section 5.3. Geomicrobiology, D-14473 Potsdam, Germany

h Ludwig-Maximilians-Universität München, Department of Earth & Environmental Sciences, Paleontology & Geobiology, 80333 Munich, Germany

Department of Microbiology and Immunology and Department of Earth, Ocean, and Atmospheric Sciences, University of British Columbia, Vancouver, Canada

<sup>&</sup>lt;sup>j</sup> Research Center for Limnology, Indonesian Institute of Sciences (LIPI), Jl. Raya Bogor, Cibinong, Bogor, West Java 16911, Indonesia

<sup>&</sup>lt;sup>k</sup> Faculty of Mining and Petroleum Engineering, Institut Teknologi Bandung, Bandung 40132, Indonesia

to these changes (Dean et al., 1997; Meyers, 1997; Meyers and Lallier-Vergès, 1999; Ariztegui et al., 2001). Fresh OM can be easily degraded by oxidation, respiration and anoxic microbially-mediated decomposition in the water column and within the sediment. The most labile organic fraction, such as microbial biomass or water-soluble OM, will be mineralized into  $CO_2$  and  $CH_4$ , and contribute to the precipitation of other mineral phases, such as carbonates (Henrichs, 1993), potentially leaving behind the most recalcitrant OM. A better understanding of the underlying processes that convert total organic carbon (TOC – in wt%) to mineral carbon (MinC – in wt%) is therefore crucial for accurate reconstructions of depositional and post-depositional environments.

Thermal analyses are especially useful since specific temperature thresholds enable the distinction between TOC and MinC. Among the most common techniques, Rock-Eval pyrolysis (Espitalié et al., 1985) provides measurements of both TOC and MinC, as well as indices that can be used towards disentangling OM sourcing: the Oxygen Index (OI) and Hydrogen Index (HI), or the g CO<sub>2</sub> and g HC per g of TOC, respectively. These indices have widely been used to discriminate between sources of OM in previous studies (e.g., Tyson, 1995; Meyers, 1997; Meyers and Lallier-Vergès, 1999) and enabled, for example, the reconstruction of variations in authigenic biomass as a result of climate change (Ariztegui et al., 2001; Steinmann et al., 2003) and erosional patterns in subalpine sediments due to anthropogenic impact (Giguet-Covex et al., 2011; Bajard et al., 2017).

To achieve these results, the Rock-Eval analyser (Vinci, France) performs a pyrolysis of the samples to 650 °C, followed by combustion to 850 °C, with hydrocarbons, CO and CO<sub>2</sub> measured during the thermal decomposition of OM and carbonate minerals. The main advantage of the Rock-Eval method lies in the simple and fast sample preparation, and the simultaneous determination of TOC, MinC, and of indices enabling the qualitative (OM sourcing & degradation) characterization of OM. However, the presence of siderite (FeCO<sub>3</sub>) in samples is known to impact the accuracy of standard Rock-Eval parameters (Lafargue et al., 1998). The siderite-matrix effect, first mentioned by Espitalié et al. (1980), is due to the low cracking temperature of pure siderite (515-519 °C; Pillot et al., 2014) compared to other carbonates (i.e. rhodochrosite, 647-652 °C; calcite, 776-850 °C; aragonite, 762-841 °C; Pillot et al., 2014), thus overlapping the cracking temperature of OM (Carrie et al., 2012). Siderite can therefore also contribute carbon during combustion of sideritic sediments and induce a significant bias for Rock-Eval analysis in such samples. This prevents the accurate measurement of MinC and TOC, while also leading to over- and underestimations of the OI and HI indices respectively. Previous studies (Pillot et al., 2014; Milesi et al., 2016; Sebag et al., 2018) have shown that siderite matrix effects can be corrected when processing Rock-Eval thermograms (evolved gas versus temperature). Milesi et al. (2016) suggested a sideritematrix effect correction derived from Rock-Eval for Paleozoic sediments, which assumes that OM has a constant CO/CO<sub>2</sub> ratio with the excess CO<sub>2</sub> originating from siderite. However, siderite also releases variable amounts of CO during pyrolysis, with the result that the CO/CO<sub>2</sub> ratio cannot be satisfactorily assumed. A more recent study proposed a correction protocol based on thermogram analysis by means of quantifying CO and CO2 released during the thermal decomposition of siderite in Holocene tropical lake sediments (Sebag et al., 2018). Nevertheless, the deposits which Sebag et al. (2018) analyzed were homogeneous in lithology and characterized by low MinC (0.2-1.9%wt). Thus, an alternative approach needs to be developed for more complex lithologies, with variations in the nature and quantity of carbon fractions to evaluate the applicability of the Rock-Eval correction method.

The Towuti Drilling Project (TDP), carried out through the International Continental Scientific Drilling Program (ICDP), aims to

understand the climatic, biological, and geomicrobiological evolution of Lake Towuti, a part of the Malili lakes system in Indonesia, during the Pleistocene (Russell et al., 2016). Here, we used Rock-Eval analysis to study sediments acquired by the TDP, which have variable lithologies and abundant siderite (Russell et al., 2016). Rock-Eval data show different OM characteristics in samples where MinC values (>0.3–0.5%) indicate the presence of carbonates inducing potential matrix effects. Therefore, we used a novel End-Member Analysis (EMA) approach to deconvolve Rock-Eval thermograms and defined accurate thermal boundaries for organic and inorganic carbon. Following this step, we estimated siderite abundance and calculated matrix effect-free Rock-Eval parameters. Finally, we utilized our dataset for qualitative OM characterization, i.e. determination of sources and identification of degradation processes preceding the formation of siderite.

## 2. Local setting, sampling and lithology

#### 2.1. Study Site

Lake Towuti (2.75°S, 121.5°E, 318 m a.s.l.) is a tectonic lake located in central Sulawesi, Indonesia (Fig. 1), With a surface area of  $\sim$ 560 km<sup>2</sup> and a maximum water depth of 203 m, it is the largest of a set of five basins forming the Malili lake system. Lying within the East Sulawesi Ophiolite complex, Lake Towuti has a catchment composed primarily of ultramafic rocks (Monnier et al., 1995; Kadarusman et al., 2004). The tropical and humid climate conditions, with precipitation averaging 2700 mm yr<sup>-1</sup> (Konecky et al., 2016), leads to erosion and extensive lateritic soil formation (Morlock et al., 2018). Most of the lake is surrounded by a dense rainforest. However, a recent increase in agricultural activity, particularly in the northern part of the catchment, has led to substantial deforestation (Vuillemin et al., 2017; Morlock et al., 2018). Water chemistry is dominated by Mg<sup>2+</sup> and HCO<sub>3</sub> and low sulfate concentrations (1.5-2 ppm) with circumneutral pH (7.3-7.8). Nutrient concentrations are close to, or below, the detection limit -making Lake Towuti one of the least productive lakes on Earth (Lehmusluoto et al., 1997; Haffner et al., 2001). The water column is weakly thermally stratified, with anoxic conditions below 130 m, allowing for an enrichment of dissolved Fe<sup>2+</sup> (0.12 ppm) (Costa et al., 2015; Vuillemin et al., 2016). OM in modern sediments seems to be mainly sourced from authigenic production as shown by a C/N ratio averaging 10.8 (Meyers and Lallier-Vergès, 1999; Hasberg et al., 2018). Higher ratios, located in front of the main inlets and steep slopes, support fluvial OM supply from terrestrial sources in near shore areas.

## 2.2. Lithology and sampling

Our samples (n = 166) are derived from a drill core composite stratigraphic section of the upper 113 m of site TDP-TOW15-1 (Fig. 1), including holes 1A, 1B, 1D, and 1F. The upper  $\sim$ 100 m of sediments in this section were continuously deposited in a lacustrine environment and likely represent hundreds of thousands of years of lake history (Russell et al., 2016). Sediments below 100 m indicate deposition in shallow lacustrine, riverine, and swamp environments (Russell et al., 2016).

Lake Towuti's sediments principally consist of an alternation of two types of unconsolidated clays: green clays and red clays, the latter of which contain variable concentrations of siderite (Russell et al., 2014, 2016; Vogel et al., 2015). Mineralogical analyses of surficial sediments and shallow cores show that fine-grained sediments are primarily composed of phyllosilicates, namely serpentine, smectite and kaolinite, with variable but generally low, amounts of silt-sized siliciclastics and diverse occurrence of Fe-

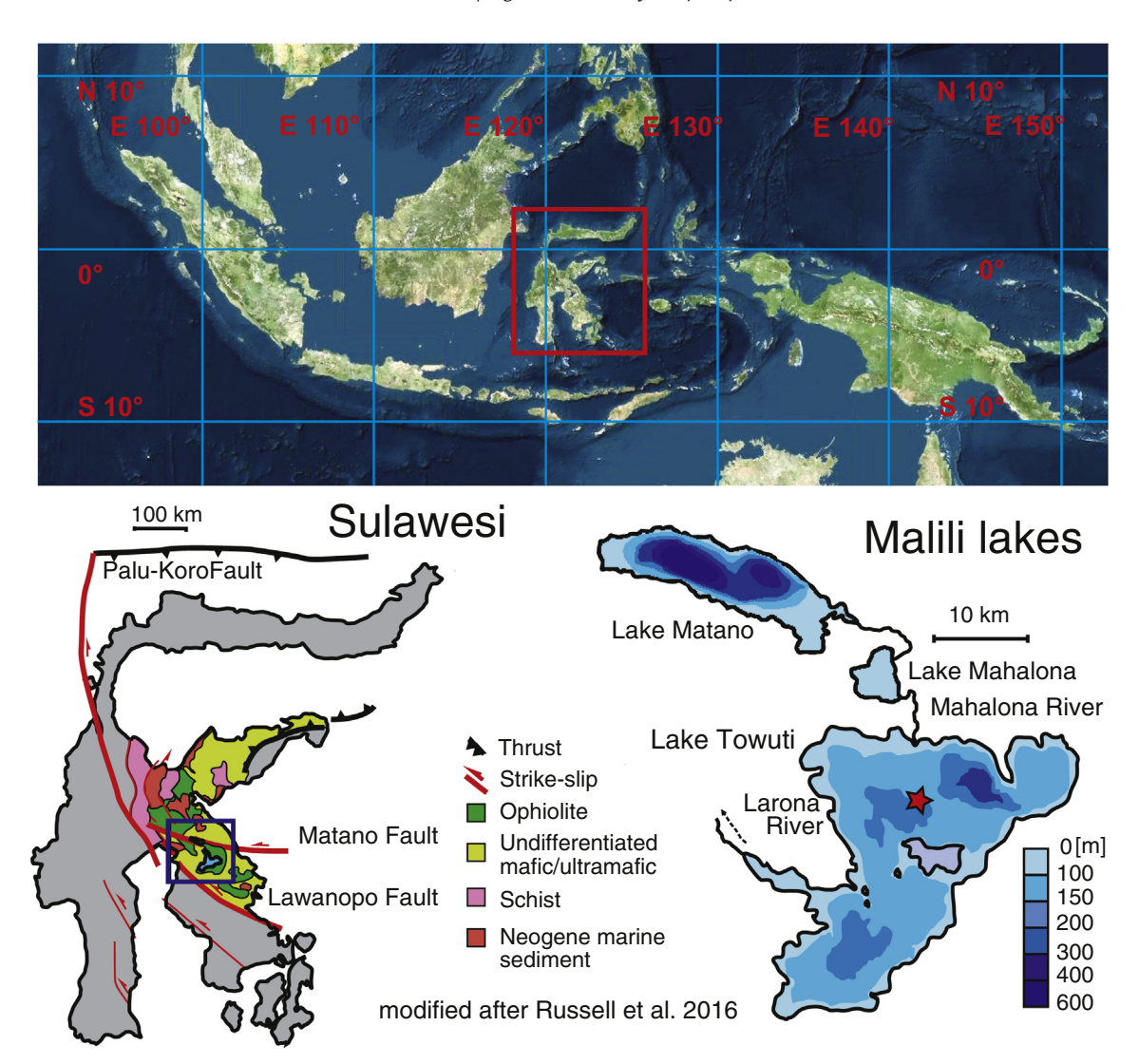


Fig. 1. Modified after Russell et al. (2014). Location of Lake Towuti within the Malili Lakes system, Sulawesi, Indonesia. The drilling site, TDP Site 1, is indicated by the red star. (For interpretation of the references to colour in this figure legend, the reader is referred to the web version of this article.)

phases such as siderite, magnetite and Fe<sup>3+</sup>-oxides (Tamuntuan et al., 2015; Vogel et al., 2015; Goudge et al., 2017; Hasberg et al., 2018; Morlock et al., 2018). Fine-grained pelagic sediments in the core are occasionally interspersed with coarser grained turbidites and concretionary levels rich in siderite (Russell et al., 2016). Despite the low primary productivity today, OM can be abundant in larger quantities, such as the few diatomaceous lithologies, which have been observed at depth in the cores (Russell et al., 2016).

## 3. Methods

#### 3.1. The Rock-Eval method

All samples were freeze-dried and homogenized using a mortar and pestle. Rock-Eval analyses were performed with a Rock-Eval 6 pyrolyser (Vinci Technologies) at the Institute of Earth Sciences of the University of Lausanne (Switzerland). Between 55 and 70 mg of freeze-dried and powdered sample material were placed in Incoloy crucibles for analyses. The Rock-Eval analytical process consists of two sequential heating steps under different ambient conditions (Espitalié et al., 1985; Lafargue et al., 1998; Behar et al., 2001) while recording the different volatile fractions of the OM as a func-

tion of the increasing temperature. The first step is pyrolysis under an inert atmosphere (N2). Free hydrocarbons (HC) are first released isothermally at 200 °C for 3 min and measured as signal S1 (expressed in mg HC  $\rm g^{-1}$  sediment) by a flame ionization detector (FID). Samples are then progressively heated up to 650 °C at a rate of 25 °C min<sup>-1</sup>. Long-chained C-compounds and kerogen, crack and release HC, which is recorded as the S2 fraction (mg HC g<sup>-1</sup> sediment, Fig. 2A). Hydrocarbons released during these steps are measured by a flame ionization detector (FID), and the abundance of hydrocarbons measured as a function of time is called a thermogram. Simultaneously, the cracking of kerogen and OM also releases carbon dioxide (CO<sub>2</sub>) and carbon monoxide (CO) which are measured by an infrared-cell (IR). Carbon oxides' thermograms are expressed in mg CO<sub>2</sub> and mg CO per g of sediment, respectively (Fig. 2), and are referred to as S3 and S3CO. Using the S1, S2, S3 and S3CO thermograms, the pyrolysed carbon (PC, wt%), or the fraction of TOC which is proportional to the amount of hydrogen and oxygen in the OM, is measured. The second step in the Rock-Eval method is a combustion under oxidative conditions  $(N_2/O_2)$ : 80/20). Following a short cooling step, samples are progressively reheated from 300 up to 850 °C. The combusted CO is recorded as the S4CO thermogram and CO2 as S4CO2 and S5. Both oxides are measured (by IR) to quantify the residual fraction of the TOC,

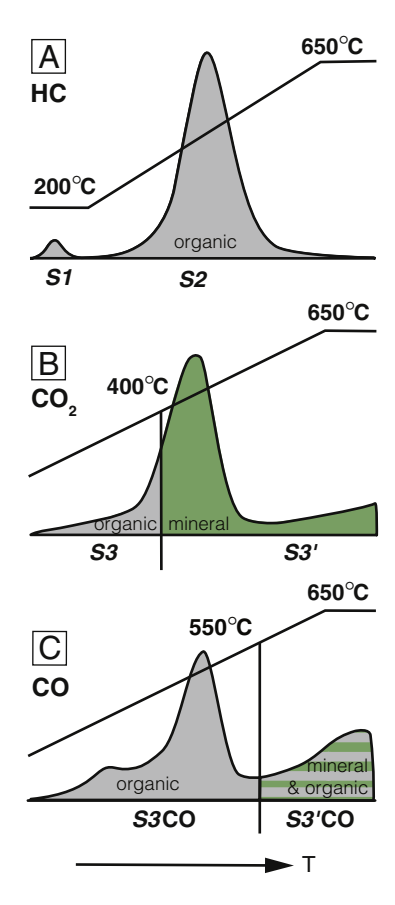


**Fig. 2.** Standard Rock-Eval temperature ranges for HC (A), CO<sub>2</sub> (B) and CO (C) thermograms in Lake Towuti sediments, modified after Behar et al. (2001). The illustration explains how intensities are conventionally split into organic and mineral carbon integrals.

referred to as residual carbon (RC – wt%), which requires external oxygen to be combusted and volatilized. Low PC/RC ratios are typical of OM rich in long-chained carbon polymers, such as organic compounds of vascular plants (Meyers, 1997; Carrie et al., 2012),

or residual/degraded OM (Henrichs, 1993). While the measured HC is exclusively of organic origin, carbonates also contribute to the production of CO<sub>2</sub> and CO within the S3 fraction, with different cracking temperatures depending on their composition (Pillot et al., 2014).

Standard Rock-Eval parameters (TOC; MinC; HI; OI) and the OI<sub>RE6</sub> (a variety of OI, calculated in mg O<sub>2</sub> g<sup>-1</sup> TOC) were calculated from thermograms using the areas between boundary temperatures based on the empirically determined equations of Lafargue et al. (1998; Table 1). The thermal boundary between organic and mineral carbon in CO<sub>2</sub> thermograms from the first step is set at 400 °C (Lafargue et al., 1998), below which CO2 is considered to be of organic origin (S3, Fig. 2B). Above 400 °C, CO<sub>2</sub> is considered to have a mineral origin (S3', Fig. 2B). Conversely, the thermal boundary in CO thermograms is variable and defined where a minimum of CO-intensity is observed (400-600 °C). If no minimum could be measured, 550 °C is taken as a default value (Fig. 2C). At lower temperatures CO intensities are considered exclusively organic (signal S3CO, Fig. 2C). As temperature increases, CO additionally evolves from the reaction of CO<sub>2</sub> with residual organic carfollowing the Boudouard equilibrium  $(CO_2 + C \leftrightarrow 2CO; Lafargue et al., 1998)$ . At high temperatures it is assumed that the CO<sub>2</sub> involved in the reaction is predominantly originating from carbonates. Therefore, above the defined minimum, CO is considered to evolve from a mixture of organic and inorganic sources (signal S3'CO, Fig. 2C).

The presence of siderite exerts a significant complication as it overlaps with the commonly used Rock-Eval thermal boundaries. This is because siderite starts to thermally decompose below 400 °C, well within the range of the cracking of OM. This challenges the use of standard Rock-Eval parameters because siderite -MinC can contribute to intensities used for the calculation of TOC and  $Ol_{RE6}$ , as well as parameters that are normalized against TOC such as the HI. However, detecting and correcting siderite effects is possible. It can be differentiated from other carbonates because it simultaneously produces both CO and  $CO_2$  at relatively low temperatures due to the additional reaction of  $CO_2$  with  $Fe^{2+}$ -oxides ( $FeCO_3 \rightarrow FeO + CO_2$ ;  $3FeO + CO_2 \rightarrow Fe_3O_4 + CO$ ). Consequently, thermograms from siderite-rich samples will show twin features on  $CO_2$  and CO thermograms (Fig. 3, simultaneous  $CO_2$  and CO peaks), whereas other carbonates will not (Espitalié et al., 1980).

Table 1 Rock-Eval parameters and their respective equations after Lafargue et al. (1998). Signals S1 and S2 correspond to HC recorded during pyrolysis.  $CO_2$  and CO from the  $C_{\rm inorg}$  fraction are given by signals S3 and S3CO.  $CO_2$  and CO from the  $C_{\rm inorg}$  fraction are given by signals S3' and S3'CO. At the oxidation step, signals S4CO<sub>2</sub> and S4CO correspond to the  $C_{\rm org}$  fraction and S5 to the  $C_{\rm inorg}$ . In grey, the revisited formulas where total intensity of CO and CO<sub>2</sub> thermograms was proportionally redistributed into organic and inorganic fractions obtained by End-Member Analysis. They replace classic signals such as S3, S3', S3CO and S3'CO.

Rock-Eval Parameter	Formula
TOC (wt%), Total Organic Carbon	PC + RC
PC (wt%), Pyrolysed Carbon	$(S1 + S2) \times 0.083 + (S3 \times 12/440) + (S3CO + 1/2S3'CO) \times 12/280$
RC (wt%), Residual Carbon	$(S4CO2 \times 12/440) + (S4CO \times 12/280)$
MinC (wt%), Mineral Carbon	PyroMinC + OxiMinC
PyroMinC (wt%)	$S3' \times 12/440 + 1/2S3'CO \times 12/280$
OxiMinC (wt%)	$S5 \times 12/440$
HI (mg HC g <sup>-1</sup> TOC), Hydrogen Index	$S2 \times 100/TOC$
OI <sub>RE6</sub> (mg O <sub>2</sub> g <sup>-1</sup> TOC), Oxygen Index	$OICO_2 \times 32/44 + OICO \times 16/28$
OI or OICO <sub>2</sub> (mg CO <sub>2</sub> g <sup>-1</sup> TOC)	$S3 \times 100/TOC$
OICO (mg CO g <sup>-1</sup> TOC)	$S3CO \times 100/TOC$
EMA-TOC (wt%)	EMA-PC + RC
EMA-PC (wt%)	$((S1 + S2) \times 0.083) + (C_{org}CO_2 \times 12/440) + (C_{org}CO \times 12/280)$
EMA-MinC (wt%)	EMA-PyroMinC + OxiMinC
EMA-PyroMinC (wt%)	$(C_{inorg}CO_2 \times 12/440) + (C_{org}CO \times 12/280)$
EMA-OI	$C_{org}CO_2 \times 100/EMA-TOC$
EMA-OICO	$C_{org}CO \times 100/EMA-TOC$
EMA-OI <sub>RE6</sub> (mg O <sub>2</sub> g <sup>-1</sup> TOC)	$(EMA-OI \times 32/44) + (EMA-OICO \times 16/28)$

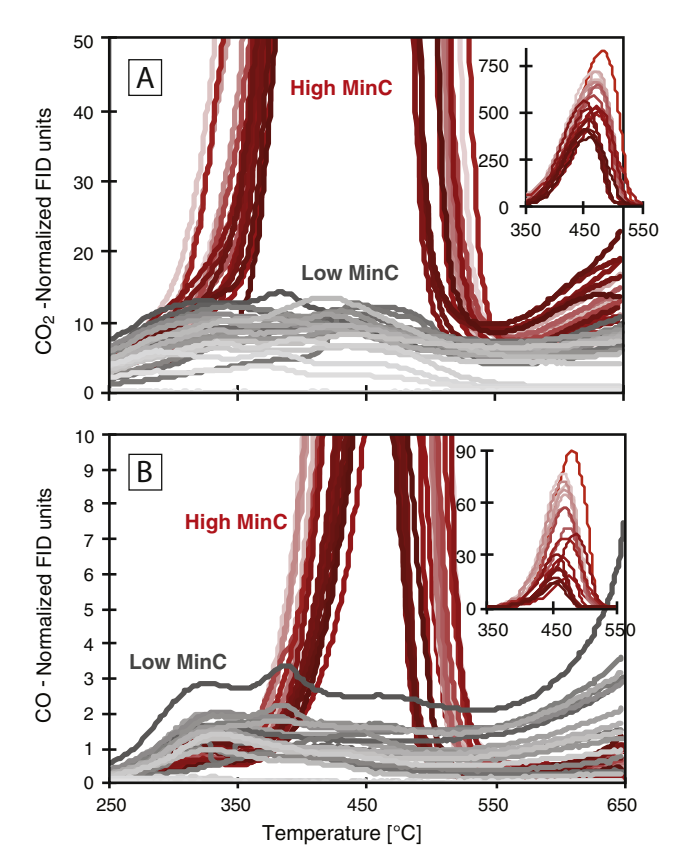


**Fig. 3.** Representative  $CO_2$  (A) and CO (B) thermograms for siderite rich (High MinC, red colors) and siderite-poor (Low MinC, grey colors) samples. The High MinC group displays high intensities between 350 and 550 °C, which corresponds to the cracking-temperature range of siderite (Espitalié et al., 1985). Intensities are normalized to sample mass. (For interpretation of the references to colour in this figure legend, the reader is referred to the web version of this article.)

Besides TOC and MinC, the Rock-Eval method allows the determination of OM quality-related indices such as HI, OI and OIREG. Plotted within a Pseudo van Krevelen diagram, they display endmembers of OM sources contributing to the sediment pool of OM preserved after deposition (Tissot and Welte, 1984; Tyson, 1995; Meyers and Lallier-Vergès, 1999). Owing to the application of Rock-Eval analysis in the context of hydrocarbon exploration, source end members are characterized as kerogen types (Tissot and Welte, 1984; Peters, 1986). Type I kerogen is rich in hydrocarbons and lipids (high HI) and is typically attributed to microbial biomass and/or the waxy coatings of leaves from land plants (Meyers, 1997; Carrie et al., 2012). Type II kerogen originates from protein-rich algal biomass. Despite a potential contribution from fresh terrestrial inputs, I and II are often considered as aquatic OM. Type III kerogen is defined by OM poor in hydrocarbons and rich in carbohydrates and lignins (main component in plant cell wall materials). It typifies woody plants, terrestrial OM, or highly degraded aquatic or terrestrial OM (Katz, 1983; Meyers and Lallier-Vergès, 1999). This typology, and in particular interpreting the source of Type III kerogen, can be ambiguous, but it hasbeen applied successfully in many paleoenvironmental studies utilizing HI and OI variations in lacustrine sediments to deduce changes in aquatic productivity and/or OM degradation in lacustrine systems (Ariztegui et al., 2001; Steinmann et al., 2003).

In addition to the previously mentioned indices typifying OM sources, two S2-derived indices; the I- and R-indices (Disnar et al., 2003; Sebag et al., 2006, 2016; Marchand et al., 2008; Albrecht et al., 2014), have been used to qualitatively characterize OM degradation. The S2 thermograms, which measure the amount

of pyrolysed HC, are normalized to 100% and divided into 5 temperature ranges, from the most thermally labile to the most thermally refractory organic fraction (A1: 280-340 °C, A2: 341-400 °C, A3: 401-460 °C, A4: 461-550 °C, A5: 551-650 °C). The Iindex (I = log [(A1 + A2)/A3]) is commonly used to assess the contribution of the most thermally labile fraction to the sedimentary OM and may be used to estimate the degree of OM preservation. Albrecht et al. (2014), showed that the I-index is sensitive to degradation of biological tissues into soil and sedimentary OM. Conversely, the R-index (R = (A3 + A4 + A5)/100) provides a qualitative measure of the thermal stability of bulk OM and can therefore be used to estimate the degree of OM degradation. Together, these indices can be used as indicators for OM degradation and mineralization. Indeed, by default, both indices are strongly inversely correlated when thermal stability is driven by preferential mineralization of the labile fraction; i.e. when the refractory fraction increases at the expense of the labile fraction during the degradation of OM.

#### 3.2. X-ray diffraction and elemental CHNS analysis

To confirm the presence or absence of siderite in samples with high and low MinC values, we performed X-ray diffraction (XRD) analyses on freeze-dried and powdered bulk sediment samples, with detection limits fluctuating between 0.2 and 0.5 wt% of MinC (Table S1 – supplementary material – Fig. A1). Whole sediment compositions were determined using a Thermo Scientific ARL X-TRA diffractometer at the Institute of Earth Sciences (University of Lausanne, Switzerland), following the methods described by Adatte et al. (1996). Reported intensities of siderite were observed at  $2\theta = 32^{\circ}$ .

Additionally, total carbon (TC) and TOC, were measured on 6 samples, covering the range of TOC and MinC values inferred by Rock-Eval analyses (Table S1, Figs. A2 and A3), with a Carlo Erba EA 1108 Elemental Analyser at the Institute of Geological Sciences, University of Bern, to evaluate the Rock-Eval dataset before and after EMA. Inorganic carbon was removed using 1 M HCl at 70 °C prior to TOC content determination. Total inorganic carbon (TIC) was calculated as the difference between TC and TOC.

## 3.3. End-Member Analysis

Thermal boundaries used in the equations for the determination of Rock-Eval parameters (Lafargue et al., 1998) were empirically defined considering the cracking temperature ranges of organic and inorganic carbon phases. The accuracy of the empirically determined thermal boundaries was tested in this study using End-Member Analysis (EMA). In particular, EMA was applied to better constrain the contribution of siderite C to quantify the MinC.

We used AnalySize, a Matlab-based Graphic User Interface typically used for processing and unmixing of grain-size distribution data (Paterson and Heslop, 2015). We followed a Single-Specimen Unmixing (SSU) method, which unmixes individual grain-size distributions (GSD) into unimodal parametric distributions using a least squares approach. Applications of EMA on GSD are commonly used to characterize sediment transport processes. Thermograms are in many ways similar to grain-size distribution spectra. This is because they consist of overlapping peaks resulting from OM and mineral carbon phases cracking at variable temperature ranges. Likewise to its application on GSD, EMA on Rock-Eval thermograms may facilitate unmixing of the thermograms into carbon endmembers and help to qualitatively characterize carbon composition in sediments.

There are two main constraints with SSU. The statistical approach presumes that intensities can be described as a linear mixture of the end-member components in which the abundances

of each end-member must be nonnegative and sum to one (100%) (Paterson and Heslop, 2015). CO and  $CO_2$  intensities in thermograms are already nonnegative values. To allow our dataset to sum to one, thermograms were normalized to 100%, i.e. intensities at each temperature increment (°C) of each thermogram were divided by the integral of the entire signal (200–650 °C).

The parametric EMA was applied to CO and CO<sub>2</sub> thermograms using a lognormal distribution fit. Thermograms measured at the oxidation step (S4CO, S4CO<sub>2</sub>, S5; Table 1) were not considered for EMA since all siderite should have been degraded during the pyrolysis stage (Espitalié et al., 1985). This is clearly visible in thermograms (Fig. 3) with siderite intensities negligible after 550 °C.

Each end-member's intensity was integrated and included in the equations of Rock-Eval parameters (Behar et al., 2001). Results of EMA and in particular the resulting relative amounts of siderite in our samples, were compared to the parameters obtained via the Rock-Eval classic thermal boundaries.

#### 4. Results

#### 4.1. Uncorrected standard Rock-Eval parameters

TOC ranges between 0.18 and 6.05 wt% (Table S2, supplementary material), which is within the range of modern surface sediments (0.17 and 6.43 wt%; Hasberg et al., 2018). RC (residual carbon) values are generally higher than PC (pyrolysed carbon), barely reaching PC/RC ratios > 1. Only 18 out of the 166 samples have a PC/RC > 1. MinC ranges between 0.11 and 4.65 wt%.

HI (15–300 mg HC  $\rm g^{-1}$  TOC) is positively related to the TOC content. OI and OI<sub>RE6</sub> are very high, reaching values above 1000 mg CO<sub>2</sub> and mg O<sub>2</sub>  $\rm g^{-1}$  TOC, respectively, especially where TOC contents are below 2 wt% (Table S2). Such high values are comparable to those reported (up to 1500 mg O<sub>2</sub>  $\rm g^{-1}$  TOC) from Gabonese lake sediments with a relatively high contribution of sand and charcoal (Sebag et al., 2013). The I index, an estimate of the preservation of the labile OM, ranges between -0.61 and 0.56. Conversely, the R index, representing the relative abundance of the thermally stable (refractory) OM, ranges between 0.50 and 0.89 (Table S2).

#### 4.2. Siderite content and matrix effect

XRD measurements confirmed macro- and microscopic observations of the presence and absence of siderite. Siderite was systematically detected by XRD in samples with variable MinC

(0.5-3 wt%, Fig. 4). However, siderite was only occasionally detected at MinC values < 0.5 wt% (i.e. 0.3 wt%, Fig. 4). Although XRD cannot provide precise estimates of siderite content, the comparison of XRD peak intensities with the Rock-Eval MinC shows very good agreement ( $R^2 = 0.91$ , Table S1) and both values are positively correlated. Moreover, other carbonate minerals were not detected by XRD. It can therefore be assumed that MinC originates from siderite while other carbonate phases are either absent or below the detection limit of XRD. This is in good agreement with previous combustion tests (Pillot et al., 2014), which show that the amount of siderite is proportional to the signal of  $CO_2$  and CO thermograms, used in the calculation of MinC.

As revealed by previous studies (Espitalié et al., 1985; Sebag et al., 2018), siderite can contribute to the S3 and S3CO integrals (used to calculate the PC and TOC; Table 1). This affects Rock-Eval TOC and MinC assessment and can strongly bias the calculation of OI and OI<sub>REG</sub> values which are particularly sensitive to these matrix effects on S3 and S3CO thermograms. Lake Towuti sediments with low TOC and high siderite content are particularly prone to these siderite-induced matrix effects and therefore require an evaluation and eventually a correction prior to calculating Rock-Eval parameters. To determine objectively whether siderite is accountable for the assumed matrix effects, we followed an approach totally independent of the lithological facies and focused only on our Rock-Eval thermograms. Thus, we divided the entire dataset into two groups using the median (0.31 wt%) of MinC: high *MinC* (siderite-rich samples) and *low MinC* (siderite-poor samples). This was done under the assumption that in Lake Towuti sediments MinC calculated from uncorrected Rock-Eval thermograms indicates the presence of siderite as suggested by the correlation of MinC with the XRD intensity peaks at 32.1°. The CO<sub>2</sub> and CO thermograms of the high MinC group show high intensities between 350 and 550 °C, whereas intensities in this temperature range are low in the low MinC sample set (Fig. 3). These observations are also consistent with Pillot et al. (2014) and Sebag et al. (2018) who demonstrated strong correlation between siderite content and intensity at these temperature ranges in Rock-Eval thermograms.

Based on the grouping assigned to the Lake Towuti sample set, oxygen indexes (OI and OI<sub>RE6</sub>) and TOC, two parameters sensitive to siderite effects on S3 and S3CO integrals also reveal two distinct populations related to siderite abundance (Fig. 5A and B). While both parameters present an outstanding correlation in the *low MinC* group, those of the *high MinC* spread out, particularly in

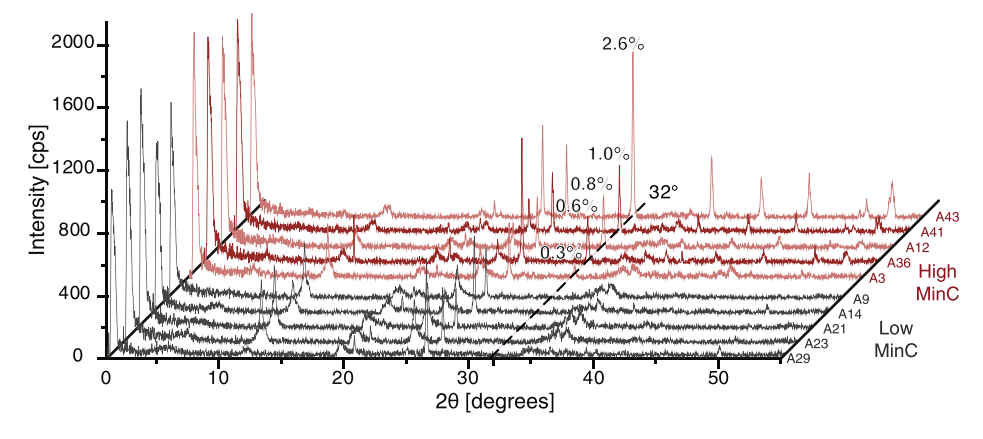
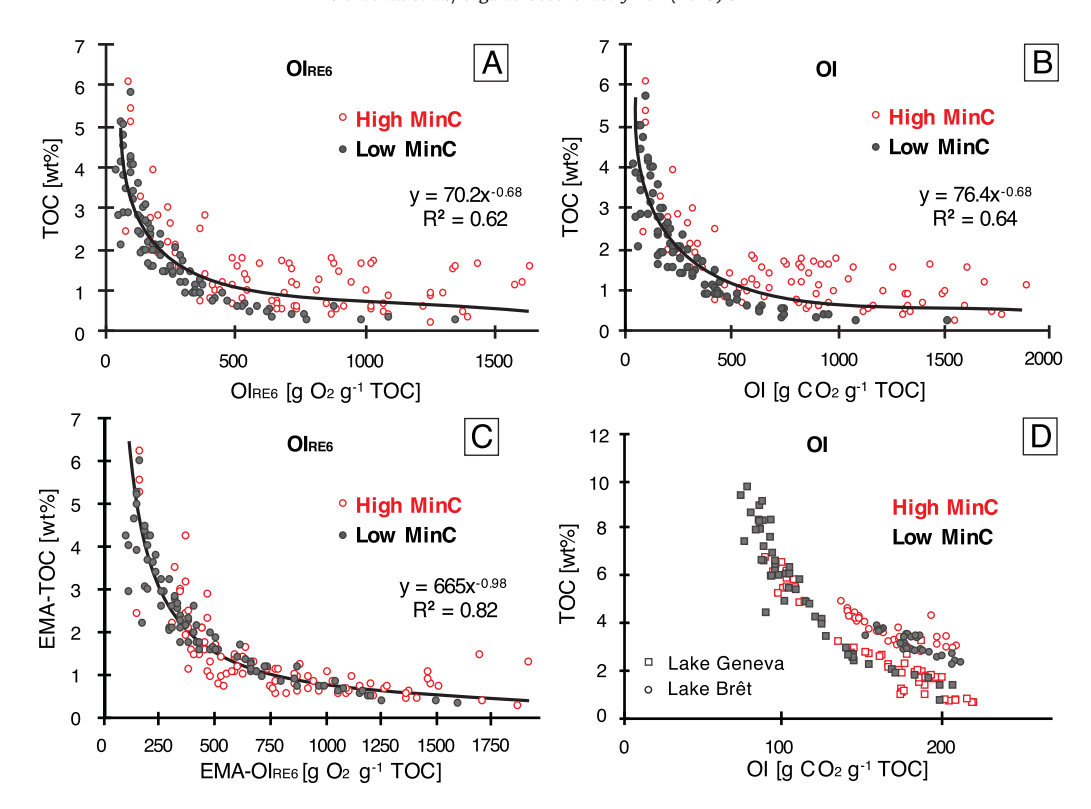


Fig. 4. X-ray diffractograms of samples from the High MinC (MinC > 0.3%) and Low MinC (MinC < 0.3%) groups showing the presence or absence of the characteristic siderite diffraction at  $2\theta = 32^{\circ}$ .



**Fig. 5.** High MinC (siderite-rich) and Low MinC (siderite-poor) samples reveal different TOC vs. OI<sub>RE6</sub> (A) and TOC vs. OI (B) properties. (C) With End-Member Analysis (EMA), the trend defined by TOC vs OI<sub>RE6</sub> is tight-clustered whether samples contain high or low/no siderite. (D) Scatterplot of TOC vs. OI presents tight clustering in lakes with low/no siderite (Lake Geneva, Gascón Díez et al., 2017; Lake Brêt, Thevenon et al., 2013). MinC in these systems is principally composed of calcite. Note the different scales in the different panels.

samples with TOC < 2 wt%. This suggests possible matrix effects on OI,  $\rm OI_{RE6}$  and TOC.

#### 4.3. Carbon distribution by End-Member Analysis

We tested different parametric distributions and optimized the linear independence of the end members (EM) by choosing the lowest maximum squared linear correlation factors (R<sup>2</sup>) between the different fitted EM. Indeed, a low linear correlation between end members is convenient since high EM correlation is an indication of overfitting where one end member is a near duplicate of another (Paterson and Heslop, 2015).

A lognormal parametric distribution in  $CO_2$  thermograms with 6 EM accounted for a specimen median  $R^2$  value of 98.6% and a maximum EM linear correlation of  $R^2$  = 0.07. The same parametric distribution in CO thermograms with 5 EM accounted for a specimen median  $R^2$  value of 95.8% with a maximum EM linear correlation of  $R^2$  = 0.20.

Using alternative parametric distributions and/or forcing the analysis to fewer or more EM, did not improve the EM linear correlation factors.

Considering a temperature of  $380-560\,^{\circ}\text{C}$  for siderite and the temperature peaks given by the algorithm, two EM in the CO and three EM in the CO<sub>2</sub> thermograms were assigned to inorganic carbon (Fig. 6A). Deconvolution of the siderite signal of CO and CO<sub>2</sub> thermograms ito 2 (at 444  $^{\circ}\text{C}$  and 473  $^{\circ}\text{C}$ ) and 3 (at 419  $^{\circ}\text{C}$ , 450  $^{\circ}\text{C}$  and 479  $^{\circ}\text{C}$ ) peaks respectively, could be the result of a thermal shift-matrix effect caused by carbonate mass variations, different degrees of crystallinity, or other mineral matrix effects (Espitalié et al., 1980; Marchand et al., 2008; Pillot et al., 2014; Kang et al., 2015).

Pillot et al. (2014) combusted rocks containing different degrees (5–40 mg) of pure siderite under oxidative conditions and sug-

gested mass variations as having a small effect in the temperature at which they release their maximum of  $CO_2$  (515–519 °C). However, the content of siderite in Lake Towuti sediments seems to influence considerably its peak of cracking temperature. Indeed, samples with MinC values > 1 wt% show that  $CO_2$  intensity peaks with a mineral origin evolve in temperature with varying MinC at a rate of ca. 12 °C per 1 wt% of MinC ( $R^2$  = 0.7; Table S3). Considering the mass range of the samples (55–70 mg) and the molar mass of siderite (115.8 g mol<sup>-1</sup>) this corresponds to rates between 1.8 and 2.3 °C mg<sup>-1</sup> of siderite, respectively.

The temperature peaks at which siderite decomposes in our samples are considerably lower than those found by Pillot et al. (2014) who combusted the carbonates (i.e. under oxidative conditions). Marchand et al. (2008) tested the decomposition of pure siderite and rhodochrosite under pyrolysis conditions and obtained results similar to those of Pillot et al. (2014) suggesting, hence, that oxidative conditions will not particularly shift the peak at which carbonates decompose. It is likely that crystal size neither has a substantial impact on the temperature at which carbonates decompose. Indeed, it has been demonstrated (Pillot et al., 2014) that different crystal sizes of pure calcite (chalk and marble) changed the temperature of maximal release of  $\mathrm{CO}_2$  by only 2–4 °C.

Conversely, other mineral matrix-effects might considerably impact the cracking of carbonates. Experimental thermal decomposition of pure siderite (Marchand et al., 2008) or siderite within a rock matrix (Pillot et al., 2014) occurs above 510 °C. Carbonates within a clayey matrix decompose at a lower range, between 400 and 475 °C (Marchand et al., 2008; Sebag et al., 2018; this study). Moreover, the presence of Fe-oxides might reduce the thermal stability of siderite by more than 100 °C (Kang et al., 2015). Sediments in Lake Towuti and many other tropical environments (Sebag et al., 2018) contain abundant Fe-oxides thus making a shift towards lower siderite decomposition temperatures more likely. Addition-

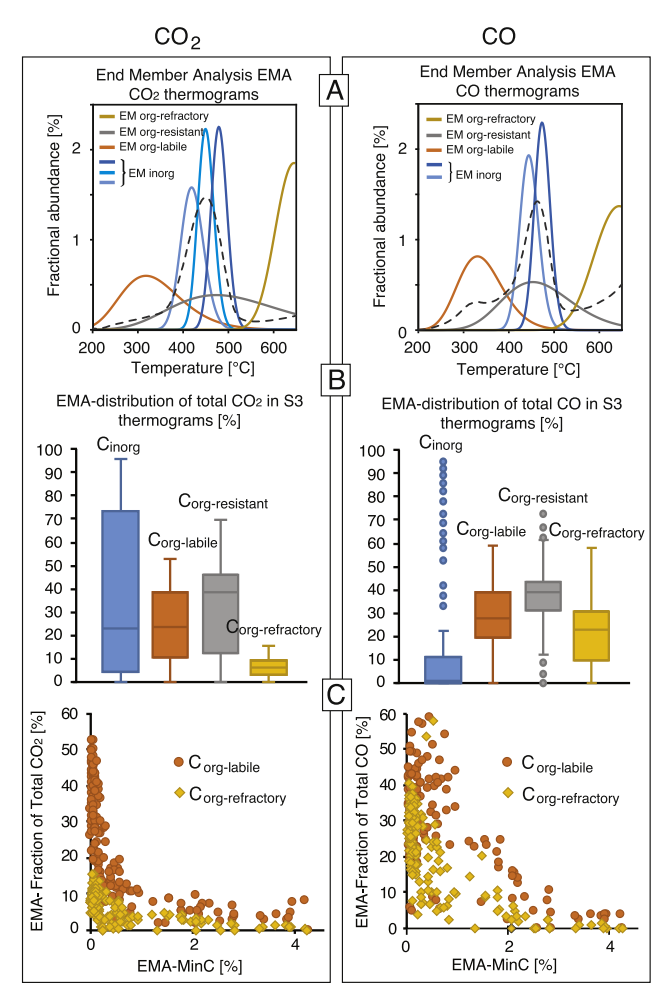


**Fig. 6.** Results of the End Member Analysis (EMA) performed on thermograms to identify and quantify carbon phases. (A) End-Members (EM) density obtained by EMA in  $\text{CO}_2$  and CO thermograms. Three and two EM, respectively, were assigned to siderite. Three End-members were attributed to organic phases. Dashed lines indicate the relative average intensity of thermograms. (B) EM were identified as siderite ( $\text{C}_{\text{inorg}}$ ), labile  $\text{C}_{\text{org}}$  ( $\text{C}_{\text{org-labile}}$ ), refractory  $\text{C}_{\text{org}}$  ( $\text{C}_{\text{org-refractory}}$ ), and an intermediate  $\text{C}_{\text{org}}$  phase moderately refractory ( $\text{C}_{\text{org-intermediate}}$ ). Integrated intensities were included in the equations of Rock-Eval parameters (Behar et al., 2001) such as MinC and TOC. (C)  $\text{C}_{\text{org-labile}}$  and  $\text{C}_{\text{org-refractory}}$  are both negatively correlated to the MinC calculated by EMA (EMA-MinC) suggesting consumption of both  $\text{C}_{\text{org}}$  phases. However,  $\text{C}_{\text{org-labile}}$  is generally more abundant than  $\text{C}_{\text{org-refractory}}$  even at high MinC, indicating resilience of  $\text{C}_{\text{org-labile}}$  to mineralization processes.

ally, SEM-EDX analyses of siderite in Lake Towuti sediments show substitution of Fe by Mn with an average Mn atomic/Fe atomic of 0.13 (Vuillemin et al., 2019). Since rhodochrosite decomposes at higher temperatures (Marchand et al., 2008; Pillot et al., 2014), its presence could also explain some of the variability of the cracking temperature of siderite.

The three remaining EM in CO (peaks at 331 °C, 453 °C and 644 °C) and CO<sub>2</sub> (peaks at 317 °C, 473 °C and 646 °C) thermograms were assigned to organic carbon. Considering the different temperature peaks of the EMs and the thermal properties of OM, we indexed them as labile organic carbon ( $C_{\rm org-labile}$ ), resistant organic carbon ( $C_{\rm org-resistant}$ ), and refractory organic carbon ( $C_{\rm org-refractory}$ ) (Fig. 6A). Intensities of EM attributed to siderite were combined and indexed as inorganic carbon ( $C_{\rm inorg}$ ). In light of the EMA results, The  $C_{\rm org-resistant}$  appears to be a substantial source of CO and CO<sub>2</sub> in pyrolysis (Fig. 6B). However, CO and CO<sub>2</sub> in some sediments are almost exclusively derived from carbonates. The  $C_{\rm org-refractory}$  has as well an important contribution, possibly enhanced by the interaction with Fe-oxides (Grand et al., 2018).

EMA-derived organic and inorganic carbon in CO and CO<sub>2</sub> thermograms were used to calculate TOC (EMA-TOC), MinC (EMA-MinC), and Rock-Eval indices (EMA-HI and EMA-OI<sub>RE6</sub>). Briefly, the total intensity of CO and CO<sub>2</sub> thermograms was proportionally redistributed into organic and inorganic moieties based on the discriminatory EM's (C<sub>org</sub>CO<sub>2</sub> and C<sub>inorg</sub>CO<sub>2</sub>; C<sub>org</sub>CO and C<sub>inorg</sub>CO), replacing classic CO<sub>2</sub> and CO signals (S3 and S3'; S3CO and S3'CO). EM based values were then included in the standard formulas (Table 1) to calculate Rock-Eval parameters.

The Boudouard effect, assuming CO above 550 °C as half organic and half mineral (Fig. 2), was not considered in calculations because (1) siderite is thought to be entirely consumed above 550 °C; (2) the effect is negligible below 550 °C (Espitalié et al., 1985); and (3) other carbonates are absent. Therefore, all CO from  $C_{\text{org-refractory}}$  peaks is assumed as exclusively organic.

## 4.4. Rock-Eval thermal boundaries by End-Member Analysis

Parameters obtained using EMA are in agreement (Table S1) with those obtained with classic Rock-Eval thermal boundaries although there are slight differences in the TOC and MinC distribution between both approaches. EMA-TOC concentrations (0.70–6.22 wt%) increased by up to 0.39 wt% at the expense of the EMA-MinC (0.01–4.26 wt%), suggesting an overestimation of the initial MinC. This overestimation is almost exclusive to samples with MinC < 1 wt%. Samples with MinC > 1 wt% are usually underestimated. Additionally, using EMA allowed constraint of MinC values of zero. This is consistent with lithological observations in most of the green clays, where siderite is absent. EMA-OI values range from 109 to 2392 mg CO<sub>2</sub> g<sup>-1</sup> TOC and EMA-OI<sub>REG</sub> values are comprised between 110 and 1872 mg O<sub>2</sub> g<sup>-1</sup> TOC, much higher than values obtained using conventional Rock-Eval thermal boundaries.

In any case, both approaches produce OI and OIRE6 values that are exceptionally high and exceed by far those of previously reported values (up to  ${\sim}500\,\text{mg}$  CO $_2$  g $^{-1}$  TOC) in studies carried out in diverse environments (Meyers and Lallier-Vergès, 1999; Li et al., 2000; Steinmann et al., 2003; Vannière et al., 2008; Debret et al., 2014; Omodeo-Salé et al., 2016). These studies have similar and coherent OI values, suggesting a specific type of OM even though their settings are different. Conversely, very high OI<sub>RE6</sub> values (up to 1500 mg O<sub>2</sub> g<sup>-1</sup> TOC) have been reported (Sebag et al., 2013; Mabicka Obame et al., 2014) in tropical environments and thus possibly indicate highly degraded OM. OIREG values higher than  $1000 \text{ mg } O_2 \text{ g}^{-1}$  TOC have as well been reported in C horizons from cambisols in mountain areas where OM is scarce and strongly degraded (Giguet-Covex et al., 2011; Bajard et al., 2017). Despite the high values, EMA-OI<sub>RE6</sub> correlate very well with EMA-TOC (Fig. 5C) and the High and Low MinC constitute this time a more tightly clustered single group as is the case in samples with low or no siderite from one Alpine (Lake Geneva; Gascón Díez et al., 2017) and one artificial lake in Switzerland (Lake Brêt; Thevenon et al., 2013; Fig. 5D). This suggests that EMA-derived Rock-Eval parameters are widely unbiased by siderite matrix effects.

## 5. Discussion

5.1. End-Member Analysis for siderite matrix effect-free Rock-Eval parameters

TOC, MinC, and Rock-Eval indices for OM characterization calculated from uncorrected Rock-Eval thermograms are clearly affected by siderite matrix effects in Lake Towuti sediments. Our approach corrects these Rock-Eval matrix induced biases, improves estimates of OM content in sediments, and optimizes indices used

for OM characterization. Here we used the TOC vs. OI<sub>RE6</sub> scatterplot as a matrix effect proxy. Samples with low or no siderite have an exponential relationship with tight clustering (*Low MinC*, Fig. 5A) as previously shown in other lacustrine environments containing low or no siderite (Fig. 5D; Thevenon et al., 2013; Gascón Díez et al., 2017). Samples with an excess or deficiency in CO<sub>2</sub> with a siderite origin spread out in a much looser clustering (*High MinC*; Fig. 5A) as for Lake Towuti sediments containing siderite. The improvements from our EMA correction on TOC and OI<sub>RE6</sub> values are clearly demonstrated in Fig. 5C, where the relation of TOC with OI<sub>RE6</sub> for High and Low MinC samples is similar after correction.

In Lake Towuti, siderite matrix effects only affect TOC moderately- since most of the TOC (76% for Low MinC and 72% High MinC) is composed of RC, which is not affected by matrix effects because it is measured during the oxidation step. This emphasizes that the co-pyrolysis of siderite and most of the OM is limited and that the overlap of signals is low. Conversely, some PC values, the fraction of TOC (24% for Low MinC and 28% High MinC) measured during the pyrolysis step, were corrected for matrix effects and increased at the expense of MinC, after EMA. The underestimation of PC values can be explained by the limit set at 400 °C by the conventional approach to split the organic and inorganic carbon pools (Fig. 2), despite the refractory OM pyrolysing above that limit (Fig. 6) and even beyond 550 °C, as shown in our thermograms (Fig. 3). This is why MinC is overestimated when its values are lower than 1 wt%. Conversely, if siderite is abundant (MinC > 1 wt%), intensities below 400 °C are high enough to trigger a bias, and as a result MinC is underestimated. Moreover, EMA showed an abundant Corg-resistant component (32% of total CO2 and 35% of total CO) in Lake Towuti sediments, potentially combusting along with siderite (Fig. 6). However, siderite-rich sediments in this study contain low TOC, and hence also low total Corg-resistant. Therefore, the bias is generally modest and specific to a few samples with high PC and abundant siderite. For instance, after EMA, samples with EMA-PC and EMA-MinC values > 1 wt% showed a carbon redistribution between 0.26 and 0.39 wt% (Table S2), much larger than the average correction (0.14 wt%).

The EMA routine allowed us to evaluate and better constrain TOC and MinC in samples with variable amounts of organic carbon and siderite compared to other Rock-Eval siderite-matrix effect corrections (Milesi et al., 2016; Sebag et al., 2018). Samples with low PC and abundant siderite, as is the case for the majority, present low to moderate matrix effects. However, EMA appears particularly valuable in settings where PC and MinC values are high. Moreover, our novel approach allowed us to satisfactorily estimate siderite content in Lake Towuti sediments. Based on EMA-MinC, modal concentrations of siderite in the bulk sediment range from 0 to 45 wt%, with an average of 7 wt%, which is consistent with macro- and microscopic observations. Conversely, the already high OIRE6 values considerably increased after correction. Similar increases in OI<sub>RE6</sub> after correcting carbonate matrix effects have been reported in other studies; indeed, this is expected as the correction removes carbon from estimates of TOC. For instance, Baudin et al. (2015) performed Rock-Eval analyses in Timor Sea sediments and showed simultaneous CO<sub>2</sub> production from residual carbon (RC) and poorly crystallized calcite. In that study, after correction of TOC values (0.81 wt% ± 0.04), OI increased to values as high as 750 mg CO<sub>2</sub> g<sup>-1</sup> TOC. Likewise, in this study, EMA showed that a small fraction of Corg-resistant was erroneously accounted as C<sub>inorg</sub> and TOC correction resulted in an increase of OI<sub>RE6</sub> values. Therefore, low TOC content and particularly low PC values are sufficient to generate extremely high OI values, especially in Towuti sediments which are already enriched in refractory oxygenated OM. This phenomenon was previously described as a decrease in the signal-to-noise ratio with decreasing TOC (Katz, 1983; Peters, 1986; Espitalié et al., 1985) generating a low TOC-matrix effect.

Finally, to validate Rock-Eval parameters, we measured TOC and TIC in selected samples with an Elemental Analyser (EA) and siderite intensities by XRD (c.f. section 4.2). Although MinC and TOC, before EMA, correlate very well with TIC and TOC measured by EA respectively (Table S1), the slope of the linear regression deviates from the 1:1 line (e.g., MinC = 1.23 TIC + 0.09,  $R^2$  = 0.97), suggesting systematic offsets between the two methods. Differences in Rock-Eval carbon distribution (organic versus inorganic) before and after EMA are relatively small- but still relevant considering the low OM content of some Lake Towuti lithologies. However, corrections are not large enough to have an impact on the correlation factors and the slope of Rock-Eval parameters versus those obtained by the Elemental Analyser and XRD (Table S1, Figs. A1-A3). This points to methodological inconsistencies. For instance, the EA, requires prior acidification and separate measurements to constrain the inorganic carbon content. Acidification techniques are known to partially remove labile and soluble organic matter (Marchand et al., 2008; Levesque et al., 2009; Larson et al., 2010; Brodie et al., 2011) possibly leading to an underestimation of TOC values. Conversely, using weak acids can prevent the complete dissolution of carbonates, especially siderite, which is more resistant to acid dissolution than other carbonates (Larson et al., 2010; Brodie et al., 2011; Schlacher and Connolly, 2014). This could explain why C<sub>org</sub> measurements of acidified samples are systematically lower than their equivalent TOC, obtained by pyrolysis. Although EMA could improve our Rock-Eval dataset, methodological inconsistencies are still obvious and require further investigation.

## 5.2. Sources of sedimentary organic matter in Lake Towuti

Carbonate matrix effect-free Rock-Eval parameters constitute a more reliable basis to characterize OM in lacustrine sediments. This is particularly true for HI and OI (and OI<sub>RE6</sub>) indices which, plotted in the Pseudo van Krevelen diagram (Fig. 7A), typify OM sources. Typically, OI and OIRE6 increase with OM rich in highly oxidized carbon chains whether they are transported from the catchment or formed by dehydrogenation and oxidation processes during early diagenesis (Jacob et al., 2004; Sebag et al., 2018). EMA-OI<sub>RE6</sub> in this study (110-1872 mg O<sub>2</sub> g<sup>-1</sup> TOC) reach anomalously high values, most of them far beyond the usual range to characterize OM sources (Peters, 1986) in aquatic sediments (Meyers, 1997; Meyers and Lallier-Vergès, 1999; Ariztegui et al., 2001; Steinmann et al., 2003; Baudin et al., 2015) and soils (Disnar et al., 2003). Some studies have reported high OI<sub>RE6</sub> values from lignins (800 mg O<sub>2</sub> g<sup>-1</sup> TOC; Carrie et al., 2012), C horizons in cambisols (>1000 mg O<sub>2</sub> g<sup>-1</sup> TOC; Giguet-Covex et al., 2011; Bajard et al., 2017) and predominantly clastic lake sediments with abundant terrestrial OM in lateritic environments (>850 mg  $O_2$  g<sup>-1</sup> TOC; Mabicka Obame et al., 2014; Sebag et al., 2018). However, high EMA-OI<sub>RE6</sub> values could be likely the result of other matrixeffects, which in our case subsist the carbonates matrix-effect correction and affect the EMA-OIRE6 index. For instance, Fe-oxides may interact with OM (Grand et al., 2018) and clays may exert a thermal shielding effect (Espitalié et al., 1980) with, as consequence, an increase in the temperature at which OM cracks. Espitalié et al. (1985) empirically defined OI as reliable if TOC was >2 wt% and unreliable if <0.5 wt% because low TOC, causing high OI, complicates the conventional use of OI as an indicator of OM provenance. Half of our dataset presents EMA-TOC values >1.5 wt% and can, up to a certain point, be associated to highly oxidized carbon chains. However, OIREG values should be interpreted with caution and OM characterization in similar settings requires complementary analyses such as  $\partial^{13}C$  and/or biomarkers.

Unlike  $OI_{REG}$ , EMA-HI values are within the usual range of OM characterization and were unaffected by carbonate matrix-

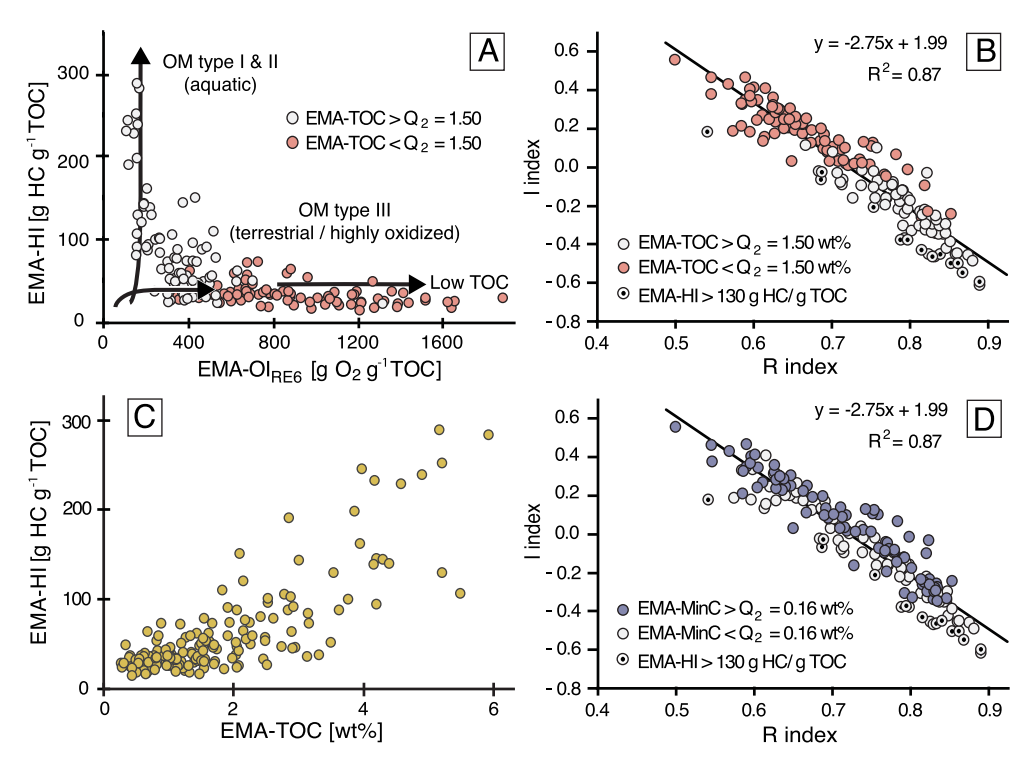


Fig. 7. (A) Pseudo van Krevelen diagram and its main endmembers typifying OM: type I and II, aquatic OM; type III, terrestrial or highly oxidized OM. Very high OI<sub>RE6</sub> values are explained by low TOC content in Lake Towuti sediments. (B) I-R diagram suggesting larger degradation in samples with higher EMA-HI and EMA-TOC values. (C) EMA-TOC vs. EMA-HI showing linear dependence at TOC contents between 1 wt% and 6 wt%. (D) I-R diagram suggesting degradation independent of the EMA-MinC.

effects. The entire dataset presents a relatively narrow range of EMA-HI (14–289 mg HC/g EMA-TOC), with low values consistent with allochthonous or highly oxidized OM and high values generally attributed to OM sourced from aquatic organisms (Tissot and Welte, 1984; Meyers and Lallier-Vergès, 1999). However, our EMA-HI values are still significantly lower than those of lipids characterizing algae (>500 mg HC g<sup>-1</sup> TOC; Meyers and Lallier-Vergès, 1999; Carrie et al., 2012). Therefore, samples with moderate EMA-HI values support intermittent inputs of algal lacustrine OM to a terrestrial-like bulk OM that characterizes OM preserved in Lake Towuti sediments.

HI/OI ratios < 0.5, as it is largely the case for Towuti samples (Table S2), have been assigned to terrestrial/soil OM (Carrie et al., 2012; Sebag et al., 2018), and this is consistent with highly-degraded allochthonous OM originating from lateritic soils in the Lake Towuti catchment. Additionally, 87% of Lake Towuti sediments have EMA-PC/EMA-RC ratios < 1 (Table S2) and are equivalent to those of carbohydrates (cellulose, pectin) and fresh materials such as conifer needles or tree bark (Carrie et al., 2012). Although such indicators suggest OM in Lake Towuti as being primarily of terrestrial origin, long-chained carbon polymers can also originate from the accumulation of recalcitrant phases following oxidation and diagenetic degradation of the labile fraction (Henrichs, 1993; Jacob et al., 2004).

## 5.3. Depositional environments and early diagenesis in Lake Towuti

I and R indices can indicate the preservation and degradation state of organic matter and, unlike  $Ol_{RE6}$  values, they are derived from S2 thermograms and thus unbiased by siderite and low TOC-matrix effects. In the I-R diagram (Fig. 7B), the whole dataset indicates a strong correlation between these two indices. Following Sebag et al. (2016), this correlation indicates that the thermal stability of sedimentary OM is controlled by degradation processes. Indeed, an OM mixture from different sources would generate

poorly related I-R indices (Sebag et al., 2016). Towuti water temperatures ranging between 28 and 30 °C (Costa et al., 2015) likely enhance degradation, which is further facilitated by methanogenesis, the most important OM mineralization pathway ( $444 \pm 172 \text{ mmol m}^{-2} \text{ yr}^{-1}$  of organic carbon) after burial in Towuti sediments (Friese et al., 2018; Vuillemin et al., 2018).

According to the I-R indices (Fig. 7B), degradation is more substantial in samples with high EMA-TOC. Additionally, the few samples with a clear dominant algal component (EMA-HI > 130 g HC g<sup>-1</sup> EMA-TOC) present the lowest I-index for a given R-index, suggesting substantial loss of the most labile OM, and appear more degraded than samples with low EMA-TOC. This supports different rates of OM degradation, which are particularly high in sediments with abundant algal OM (Fig. 7B). Greater productivity can explain the highest values of EMA-TOC and, if the OM is of planktonic origin, it is preferentially degraded compared to the more resistant terrestrial OM (Tyson, 1995). Moreover, EMA-HI correlates positively with EMA-TOC (Fig. 7C). A decrease of EMA-HI along with EMA-TOC suggests a loss of the labile fraction following degradation. According to previous studies (Huc et al., 1990; Tyson, 1995), HI values level out when sediments attaint optimal preservation conditions, usually at TOC values between 3 and 6 wt% for siliciclastic marine and lacustrine sediments. At that stage, HI can be used to determine eventually the nature of the original sources of lipidic material (Tyson et al., 1995). Since our HI values do not level out, optimal OM preservation conditions were not achieved in Lake Towuti sediments and our EMA-TOC versus EMA-HI indicates intense degradation of labile autochthonous OM.

Hence, buried OM in our high EMA-TOC samples is depleted in the labile and likely residually enriched in the more recalcitrant OM and thus shows a predominance of terrestrially sourced OM. This is in agreement with the moderately high EMA-OI $_{\rm RE6}$  values with a terrestrial-like signature. If extremely high EMA-OI $_{\rm RE6}$  are due to a low EMA-TOC-matrix effect, as seen in Section 5.1, moderately high EMA-OI $_{\rm RE6}$  from kerogens could be the result of

accumulation of refractory phases. However, differentiating kerogens with a terrestrial origin from those formed by in-situ degradation in samples with low EMA-HI and moderately high EMA-OI $_{\rm RE6}$  requires further investigation and possibly a detailed organic geochemical approach.

Finally, unlike EMA-TOC, EMA-MinC do not define a clear relation with the I-R indices (Fig. 7D) and degradation processes seem not to be related to the abundance of siderite. This points to a substantial contribution of siderite forming post-burial and thus after the majority of the OM has already been degraded. Indeed, according to EMA, Corg-labile and Corg-refractory both decrease with increasing Cinorg, suggesting that "labile" and "refractory" fractions are indistinctly mineralized (Fig. 6C) into intermediate phases such as CH<sub>4</sub> and CO<sub>2</sub> (Friese et al., 2018) prior to siderite formation. This brings to light different degradation processes of OM followed by a subsequent (diagenetic) transition of organic carbon to siderite (Vuillemin et al., 2019).

#### 6. Conclusion

Despite its many advantages, a potential problem with Rock-Eval analysis arises from the bias introduced by matrix effects that hamper the robust determination of  $Ol_{RE6}$ , MinC and TOC values. Samples with abundant siderite thus require a suitable matrix-correction approach to generate unbiased Rock-Eval parameters.

Using End-Member Analysis (EMA) we were able to correct Rock-Eval thermograms for siderite matrix effects allowing for a more accurate determination of widely used parameters for quantitative and qualitative organic matter characterization. Carbonate matrix effects slightly affected TOC and MinC values since the major component of the organic carbon was obtained during the oxidation step and thus was not synchronous with the pyrolysis of siderite. However, very low TOC contents, and probably the presence of clays and Fe-oxides, induced anomalously high OI<sub>RE6</sub> values, which could not be exploited using classic Rock-Eval interpretation schemes and should be interpreted with caution.

Standard Rock-Eval indices obtained by EMA combined with alternative indices derived from S2 thermograms (I-R) can be used as valuable indicators for OM sourcing and degradation in geochemically exceptional Lake Towuti sediments. The I- and R-indices suggested different degradation processes: in combination with high EMA-HI-values, they indicated an intermittent algal input to the sediments, followed by intense loss of the labile organic fraction; associated to high EMA-TOC and moderately high EMA-OI<sub>RE6</sub> they indicated strong degradation and substantial accumulation of terrestrial-like OM in the sediments. Moreover, a correlation of I-R indices with the MinC could not be determined, suggesting that the majority of OM degradation processes precede siderite formation.

In summary, our EMA-Rock-Eval approach improves identification of the sources and the intensity of degradation of OM in ferruginous and siderite bearing sediments. Due to the relatively low amount of sample preparation required and rapid analysis EMA Rock Eval approaches are particularly useful for generating high-resolution datasets for OM sourcing and quality and for targeting specific sediment intervals out of long sediment succession for more time-consuming analyses.

## 7. Dataset

Ordoñez, Luis; Vogel, Hendrik; Adatte, Thierry; Sebag, David; Ariztegui, Daniel; Russell, James; Kallmeyer, Jens; Vuillemin, Aurèle; Bijaksana, Satria; Crowe, Sean; Friese, André (2019), "Empowering conventional Rock-Eval pyrolysis for organic matter characterization of the siderite-rich sediments of Lake Towuti

(Indonesia) using End-Member Analysis.", Mendeley Data, v1 https://doi.org/10.17632/nrzksn8jzc.1.

#### Acknowledgements

The Towuti Drilling Project was partially supported by grants from the International Continental Drilling Program, the US National Science Foundation, the German Research Foundation, the Swiss National Science Foundation (20FI21\_153054/1 200021\_153053/1), Brown University, Genome British Columbia, and the Ministry of Research, Technology, and Higher Education (RISTEK). PT Vale Indonesia, the US Continental Drilling Coordination Office, the GeoForschungs-Zentrum Potsdam and DOSECC Exploration Services are acknowledged for logistical assistance to the project. This research was carried out with permission from the Ministry of Research and Technology (RISTEK), the Ministry of Trade of the Republic of Indonesia, and the Natural Resources Conservation Center (BKSDA) and Government of Luwu Timur of Sulawesi. We thank the valuable comments and suggestions of F. Baudin and Ch. Giguet-Covex to an early version of this manuscript as well as co-Editor in Chief S. Rowland.

#### **Author contribution**

L. Ordoñez (LO), D. Ariztegui (DA), D. Sebag (DS), and H. Vogel (HV) designed the study; LO sampled at LacCore, conducted laboratory analyses, led the writing of the manuscript and designed the figures. J. M. Russell (JMR), S. Bijaksana (SB), HV, and M. Melles (MM) designed and led the Towuti Drilling Project. LO, HV, JMR, SB, A. Friese (AF), J. Kallmeyer (JK), S. A. Crowe (SAC), K. W. Bauer (KWB), R. Simister (RS), A. Vuillemin (AV), and S. Nomosatryo (SN) participated in fieldwork and LO, DA, HV, JMR, JK, and AV participated in core opening. JMR and HV developed the sediment stratigraphy. T. Adatte (TA) contributed with XRD facilities and provided external data. All authors were involved in discussions about the data and contributed to writing and improving the manuscript. Members of the Towuti Drilling Project provided scientific, technical, and logistical support during field sampling and core opening.

#### Appendix A. Supplementary material

Supplementary data to this article can be found online at https://doi.org/10.1016/j.orggeochem.2019.05.002.

Associate Editor—Clifford C. Walters

#### References

Adatte, T., Stinnesbeck, W., Keller, G., 1996. Lithostratigraphic and mineralogic correlations of near K/T boundary clastic sediments in northeastern Mexico: implications for origin and nature of deposition. Geological Society of America Special Paper 307, 211–226.

Albrecht, R., Sebag, D., Verrecchia, E., 2014. Organic matter decomposition: bridging the gap between Rock-Eval pyrolysis and chemical characterization (CPMAS13C NMR). Biogeochemistry 122, 101–111.

Ariztegui, D., Chondrogianni, C., Lami, A., Guilizzoni, P., Lafargue, E., 2001. Lacustrine organic matter and the Holocene paleoenvironmental record of Lake Albano (central Italy). Journal of Paleolimnology 26, 283–292.

Bajard, M., Develle, A.-L., Arnaud, F., David, F., Giguet-Covex, C., Pignol, C., Jacob, J., Crouzet, C., Poulenard, J., Sabatier, P., 2017. Progressive and regressive soil evolution phases in the Anthropocene. Catena 150, 39–52.

Baudin, F., Disnar, J.-R., Aboussou, A., Savignac, F., 2015. Guidelines for Rock-Eval analysis of recent marine sediments. Organic Geochemistry 86, 71–80.

Behar, F., Beaumont, V., Penteado, H.L. De B., 2001. Rock-Eval 6 technology: performances and developments. Oil & Gas Science and Technology 56, 111–134.

Brodie, C.R., Casford, J.S.L., Lloyd, J.M., Leng, M.J., Heaton, T.H.E., Kendrick, C.P., Yongqiang, Z., 2011. Evidence for bias in C/N,  $\delta^{13}$ C and  $\delta^{15}$ N values of bulk organic matter, and on environmental interpretation, from a lake sedimentary

- sequence by pre-analysis acid treatment methods. Quaternary Science Reviews 30, 3076–3087.
- Carrie, J., Sanei, H., Stern, G., 2012. Standardisation of Rock-Eval pyrolysis for the analysis of recent sediments and soils. Organic Geochemistry 46, 38–53.
- Costa, K.M., Russell, J.M., Vogel, H., Bijaksana, S., 2015. Hydrological connectivity and mixing of Lake Towuti, Indonesia in response to paleoclimatic changes over the last 60,000 years. Palaeogeography, Palaeoclimatology, Palaeoecology 417, 467–475.
- Dean, W.E., Gardner, J.V., Piper, D.Z., 1997. Inorganic geochemical indicators of glacial-interglacial changes in productivity and anoxia on the California continental margin. Geochimica et Cosmochimica Acta 61, 4507–4518.
- Debret, M., Bentaleb, I., Sebag, D., Favier, C., Nguetsop, V., Fontugne, M., Oslisly, R., Ngomanda, A., 2014. Influence of inherited paleotopography and water level rise on the sedimentary infill of Lake Ossa (S Cameroon) inferred by continuous color and bulk organic matter analyses. Palaeogeography, Palaeoclimatology, Palaeoecology 411, 110–121.
- Disnar, J.R., Guillet, B., Keravis, D., Di-Giovanni, C., Sebag, D., 2003. Soil organic matter (SOM) characterization by Rock-Eval pyrolysis: scope and limitations. Organic Geochemistry 34, 327–343.
- Espitalié, J., Deroo, G., Marquis, F., 1985. La pyrolyse Rock-Eval et ses applications. Deuxième partie. Revue de l'Institut français du Pétrole 40, 755–784.
- Espitalié, J., Madec, M., Tissot, B., 1980. Role of mineral matrix in kerogen pyrolysis: influence on petroleum generation and migration. American Association of Petroleum Geologists Bulletin 64, 59–66.
- Friese, A., Kallmeyer, J., Glombitza, C., Vuillemin, A., Simister, R., Bijaksana, S., Vogel, H., Melles, M., Russell, J.M., Nomosatryo, S., Bauer, K., Heuer, V.B., Henny, C., Crowe, S.A., Ariztegui, D., Wegner, D., 2018. Methanogenesis predominates organic matter mineralization in a ferruginous, non-sulfidic sedimentary environment. EGU General Assembly Conference Abstracts 20, 7446.
- Gascón Díez, E., Corella, J.P., Adatte, T., Thevenon, F., Loizeau, J.L., 2017. Highresolution reconstruction of the 20th century history of trace metals, major elements, and organic matter in sediments in a contaminated area of Lake Geneva, Switzerland. Applied Geochemistry 78, 1–11.
- Giguet-Covex, C., Arnaud, F., Poulenard, J., Disnar, J.-R., Delhon, C., Francus, P., David, F., Enters, D., Rey, P.-J., Delannoy, J.-J., 2011. Changes in erosion patterns during the Holocene in a currently treeless subalpine catchment inferred from lake sediment geochemistry (Lake Anterne, 2063 m a.s.l., NW French Alps): the role of climate and human activities. The Holocene 21, 651–665.
- Goudge, T.A., Russell, J.M., Mustard, J.F., Head, J.W., Bijaksana, S., 2017. A 40,000 yr record of clay mineralogy at Lake Towuti, Indonesia: paleoclimate reconstruction from reflectance spectroscopy and perspectives on paleolakes on Mars. Bulletin of the Geological Society of America 129, 806–819.
- Grand, S., Viret, F., Sebag, D., Verrecchia, E., 2018. Rock-Eval pyrolysis of density fractions from tropical soils of Western Uganda. RST Société géologique de France. 638.
- Haffner, G.D., Hehanussa, P.E., Hartoto, D., 2001. The biology and physical processes of large lakes of Indonesia: Lakes Matano and Towuti. In: Munawar, M., Hecky, R.E. (Eds.), The Great Lakes of the World. Food-web, Health and Integrity. Backhuys Publishers, Leiden, pp. 183–192.
- Hasberg, A.K.M., Bijaksana, S., Held, P., Just, J., Melles, M., Morlock, M.A., Opitz, S., Russell, J.M., Vogel, H., Wennrich, V., 2018. Modern sedimentation processes in Lake Towuti, Indonesia, revealed by the composition of surface sediments. Sedimentology 66, 675–698.
- Henrichs, S.M., 1993. Early diagenesis of organic matter: the dynamics (rates) of cycling of organic compounds. In: Engel, M.H., Macko, S.A. (Eds.), Organic Geochemistry: Principles and Applications. Springer, pp. 101–117.
- Huc, A.Y., Le Fournier, J., Vandenbroucke, M., Bessereau, G., 1990. Northern Lake Tanganyika – an example of organic sedimentation in an anoxic rift lake, in Lacustrine Basin Exploration: case studies and modern analogs. American Association of Petroleum Geologists Memoir 50, 169–185.
- Jacob, J., Disnar, J.R., Boussafir, M., Sifeddine, A., Turcq, B., Albuquerque, A.L.S., 2004. Major environmental changes recorded by lacustrine sedimentary organic matter since the last glacial maximum near the equator (Lagoa do Caçó, NE Brazil). Palaeogeography, Palaeoclimatology, Palaeoecology 205, 183–197.
- Kadarusman, A., Miyashita, S., Maruyama, S., Parkinson, C.D., Ishikawa, A., 2004. Petrology, geochemistry and paleogeographic reconstruction of the East Sulawesi Ophiolite, Indonesia. Tectonophysics 392, 55–83.
- Kang, N., Schmidt, M.W., Poli, S., Franzolin, E., Connolly, J.A.D., 2015. Melting of siderite to 20GPa and thermodynamic properties of FeCO<sub>3</sub>-melt. Chemical Geology 400, 34–43.
- Katz, B.J., 1983. Limitations of "Rock-Eval" pyrolysis for typing organic matter. Organic Geochemistry 4, 195–199.
- Konecky, B., Russell, J., Bijaksana, S., 2016. Glacial aridity in central Indonesia coeval with intensified monsoon circulation. Earth and Planetary Science Letters 437, 15–24
- Lafargue, E., Marquis, F., Pillot, D., 1998. Rock-Eval 6 applications in hydrocarbon exploration, production, and soil contamination studies. Oil & Gas Science and Technology 53, 421–437.
- Larson, T.E., Heikoop, J.M., Perkins, G., Chipera, S.J., Hess, M.A., 2010. N-Nitrosopiperazines form at high pH in post-combustion capture solutions containing piperazine: a low-energy collisional behaviour study. Rapid Communications in Mass Spectrometry 24, 3567–3577.
- Lehmusluoto, P., Machbub, B., Terangna, N., Rusmiputro, S., Achmad, F., Boer, L., Brahmana, S.S., Priadi, B., Setiadji, B., Sayuman, O., 1997. National inventory of the major lakes and reservoirs in Indonesia. Expedition Indodanau Technical Report, Edita Oy.

- Levesque, C., Juniper, K., Planas, D., 2009. Organic matter loss during hydrochloric acid treatment of aquatic samples: implications for elemental and stable isotopic analyses. In: American Geophysical Union Fall Meeting Abstracts.
- Li, L., Keller, G., Adatte, T., Stinnesbeck, W., 2000. Late Cretaceous sea-level changes in Tunisia: a multi-disciplinary approach. Journal of the Geological Society 157, 447–458
- Mabicka Obame, R., Copard, Y., Sebag, D., Abdourhamane Touré, A., Boussafir, M., Bichet, V., Garba, Z., Guillon, R., Petit, C., Rajot, J.L., Durand, A., 2014. Carbon sinks in small Sahelian lakes as an unexpected effect of land use changes since the 1960s (Saga Gorou and Dallol Bosso, SW Niger). Catena 114, 1–10.
- Marchand, C., Lallier-Vergès, E., Disnar, J.R., Kéravis, D., 2008. Organic carbon sources and transformations in mangrove sediments: a Rock-Eval pyrolysis approach. Organic Geochemistry 39, 408–421.
- Meyers, P.A., 1997. Organic geochemical proxies of paleoceanographic, paleolimnologic, and paleoclimatic processes. Organic Geochemistry 27, 213–250.
- Meyers, P.A., Lallier-Vergès, E., 1999. Lacustrine sedimentary organic matter of Late Quaternary paleoclimates. Journal of Paleolimnology 21, 345–372.
- Milesi, V., Prinzhofer, A., Guyot, F., Benedetti, M., Rodrigues, R., 2016. Contribution of siderite-water interaction for the unconventional generation of hydrocarbon gases in the Solimões basin, north-west Brazil. Marine and Petroleum Geology 71, 168–182.
- Monnier, C., Girardeau, J., Maury, R.C., Cotten, J., 1995. Back-arc basin origin for the East Sulawesi ophiolite (eastern Indonesia). Geology 23, 851–854.
- Morlock, M.A., Vogel, H., Nigg, V., Ordoñez, L., Hasberg, A.K.M., Melles, M., Russell, J. M., Bijaksana, S., 2018. Climatic and tectonic controls on source-to-sink processes in the tropical, ultramafic catchment of Lake Towuti, Indonesia. Journal of Paleolimnology 61, 279–295.
- Omodeo-Salé, S., Suárez-Ruiz, I., Arribas, J., Mas, R., Martínez, L., Josefa Herrero, M., 2016. Characterization of the source rocks of a paleo-petroleum system (Cameros Basin) based on organic matter petrology and geochemical analyses. Marine and Petroleum Geology 71, 271–287.
- Paterson, G.A., Heslop, D., 2015. New methods for unmixing sediment grain size data. Geochemistry Geophysics Geosystems 18, 1541–1576.
- Peters, K.E., 1986. Guidelines for evaluating petroleum source rock using programmed pyrolysis. American Association of Petroleum Geologists Bulletin 70, 318–329.
- Pillot, D., Deville, E., Prinzhofer, A., 2014. Identification and quantification of carbonate species using Rock-Eval pyrolysis. Oil & Gas Science and Technology Revue d'IFP Energies nouvelles 69, 341–349.
- Russell, J.M., Bijaksana, S., Vogel, H., Melles, M., Kallmeyer, J., Ariztegui, D., Crowe, S., Fajar, S., Hafidz, A., Haffner, D., Hasberg, A., Ivory, S., Kelly, C., King, J., Kirana, K., Morlock, M., Noren, A., 2016. The Towuti Drilling Project: paleoenvironments, biological evolution, and geomicrobiology of a tropical Pacific lake. Workshop Reports, 29–40.
- Russell, J.M., Vogel, H., Konecky, B.L., Bijaksana, S., Huang, Y., Melles, M., Wattrus, N., Costa, K., King, J.W., 2014. Glacial forcing of central Indonesian hydroclimate since 60,000 y B.P. Proceedings of the National Academy of Sciences 111, 5100– 5105.
- Schlacher, T.A., Connolly, R.M., 2014. Effects of acid treatment on carbon and nitrogen stable isotope ratios in ecological samples: a review and synthesis. Methods in Ecology and Evolution 5, 541–550.
- Sebag, D., Debret, M., M'voubou, M., Obame, R.M., Ngomanda, A., Oslisly, R., Bentaleb, I., Disnar, J.R., Giresse, P., 2013. Coupled Rock-Eval pyrolysis and spectrophotometry for lacustrine sedimentary dynamics: Application for West Central African rainforests (Kamalete and Nguene lakes, Gabon). The Holocene 23, 1173–1183.
- Sebag, D., Disnar, J.R., Guillet, B., Di Giovanni, C., Verrecchia, E.P., Durand, A., 2006. Monitoring organic matter dynamics in soil profiles by "Rock-Eval pyrolysis": Bulk characterization and quantification of degradation. European Journal of Soil Science 57, 344–355.
- Sebag, D., Garcin, Y., Adatte, T., Deschamps, P., Ménot, G., Verrecchia, E.P., 2018.

  Correction for the siderite effect on Rock-Eval parameters: application to the sediments of Lake Barombi (southwest Cameroon). Organic Geochemistry 123, 126–135.
- Sebag, D., Verrecchia, E.P., Cécillon, L., Adatte, T., Albrecht, R., Aubert, M., Bureau, F., Cailleau, G., Copard, Y., Decaens, T., Disnar, J., Hetényi, M., Nyilas, T., Trombino, L., 2016. Geoderma dynamics of soil organic matter based on new Rock-Eval indices. Geoderma 284, 185–203.
- Steinmann, P., Adatte, T., Lambert, P., 2003. Recent changes in sedimentary organic matter from Lake Neuchâtel (Switzerland) as traced by Rock-Eval pyrolysis. Eclogae Geologicae Helvetiae 96, 109–116.
- Tamuntuan, G., Bijaksana, S., King, J., Russell, J., Fauzi, U., Maryunani, K., Aufa, N., Ode, L., 2015. Variation of magnetic properties in sediments from Lake Towuti, Indonesia, and its paleoclimatic significance. Palaeogeography, Palaeoclimatology, Palaeoecology 420, 163–172.
- Thevenon, F., de Alencastro, L.F., Loizeau, J.L., Adatte, T., Grandjean, D., Wildi, W., Poté, J., 2013. A high-resolution historical sediment record of nutrients, trace elements and organochlorines (DDT and PCB) deposition in a drinking water reservoir (Lake Brêt, Switzerland) points at local and regional pollutant sources. Chemosphere 90, 2444–2452.
- Tissot, B.P., Welte, D.H., 1984. Petroleum Formation and Occurrence. Springer, pp. 160–198.
- Tyson, R.V., 1995. Abundance of organic matter in sediments: TOC, hydrodynamic equivalence, dilution and flux effects. In: Sedimentary Organic Matter: Organic Facies and Palynofacies. Springer, pp. 81–118.

- Vannière, B., Colombaroli, D., Chapron, E., Leroux, A., Tinner, W., Magny, M., 2008. Climate versus human-driven fire regimes in Mediterranean landscapes: the Holocene record of Lago dell'Accesa (Tuscany, Italy). Quaternary Science Reviews 27, 1181–1196.
- Vogel, H., Russell, J.M., Cahyarini, S.Y., Bijaksana, S., Wattrus, N., Rethemeyer, J., Melles, M., 2015. Depositional modes and lake-level variability at Lake Towuti, Indonesia, during the past  ${\sim}29$  kyr BP. Journal of Paleolimnology 54, 359–377.
- Vuillemin, A., Wirth, R., Kemnitz, H., Schleicher, A.M., Friese, A., Bauer, K.W., Simister, R., Nomosatryo, S., Ordoñez, L., Ariztegui, D., Henny, C., Crowe, S.A., Benning, L.G., Kallmeyer, J., Russell, J.M., Bijaksana, S., Vogel, H., Towuti Drilling Project Science Team, T., 2019. Formation of diagenetic siderite in modern ferruginous sediments. Geology 47, 1–5.
- Vuillemin, A., Friese, A., Alawi, M., Henny, C., Nomosatryo, S., Wagner, D., Crowe, S. A., Kallmeyer, J., 2016. Geomicrobiological features of ferruginous sediments from lake Towuti, Indonesia. Frontiers in Microbiology 7. Article 1007.
- Vuillemin, A., Horn, F., Alawi, M., Henny, C., Wagner, D., Crowe, S.A., Kallmeyer, J., 2017. Preservation and significance of extracellular DNA in ferruginous sediments from Lake Towuti, Indonesia. Frontiers in Microbiology 8. Article 1440.
- Vuillemin, A., Horn, F., Friese, A., Winkel, M., Alawi, M., Wagner, D., Henny, C., Orsi, W.D., Crowe, S.A., Kallmeyer, J., 2018. Metabolic potential of microbial communities from ferruginous sediments. Environmental Microbiology 20, 4297–4313.